



Research article

UDC 69

DOI: 10.34910/MCE.135.5



Experimental evaluation of negative skin friction on floating pile in gypseous soil

A.H. Mohsen[✉], **B.S. Albusoda**

Scientific Research Commission, Baghdad, Iraq

✉ abeer.h.mohsin@src.edu.iq

abeer.mohsin2001D@coeng.uobaghdad.edu.iq

Keywords: negative skin friction, NSF, steel pile, drag load, gypseous soil

Abstract. Gypseous soils are characterized by an open structure with developed porosity and high gypsum content, which determines their metastable state. When saturated with water, a decrease in volume occurs as a result of a decrease in matrix suction and degradation of cementation bonds, leading to rapid settlement. When a pile is installed in this type of soil, this can cause negative skin friction (NSF) along its surface, which increases the load pressure and reduces the safety factor. In this study, a laboratory model was used to evaluate NSF developed along the external surface of a steel pile embedded in gypseous soil. The effect of the degree of saturation, dry unit weight, length/diameter (L/D) ratio, and relative settlement between the soil and the pile on the magnitude of NSF, which can be described as a downward drag load along the pile shaft, has been studied. The results show that NSF increases with increasing L/D ratio by 66 % at the maximum collapse potential and decreases with increasing dry unit weight and degree of saturation by 26–60 % for L/D = 15 and by 78–137 % for L/D = 10. The maximum drag load occurs with zero water content and L/D = 15.

Citation: Mohsen, A.H., Albusoda, B.S. Experimental evaluation of negative skin friction on floating pile in gypseous soil. Magazine of Civil Engineering. 2025. 18(3). Article no. 13505. DOI: 10.34910/MCE.135.5

1. Introduction

Negative skin friction (NSF) generated along the pile shaft can significantly impact engineering construction when the soil foundation is collapsible during inundation. This phenomenon may lead to a reduction in the bearing capacity of the pile foundation, an increase in the pile load, and a consequent decrease in the safety factor calculated during the design processes [1–4].

There are two types of studies that have been carried out on this subject:

a) Field studies

Despite the high costs associated with these tests and changing environmental conditions (such as variation in water table level and temperature over extended testing periods) required to generate and develop NSF, these tests provide clear insights into the behavior of piles subjected to the NSF in collapsible soils [5–9].

b) Laboratory model studies

In laboratory settings, piles with specific properties are subjected to the drag load, which is developed during inundation of the collapsible soil with water under different conditions (such as time of inundation, application of ultimate or allowable load on the pile head, and surcharge on the soil surface). In addition, some studies have explored methods to reduce NSF by coating the pile shaft with bituminous materials [10–13].

Recent research has advanced the understanding of pile-negative friction in loess soil, which is one of the most important types of collapsible soil [14, 15]. Other studies have focused on artificial collapsible soils, such as sand-kaolin mixtures with varying clay and water content.

The centrifuge model tests for both single and group pipe piles, installed in sandy saturated soil with dry density ranging from 1.249 to 1.682 gm/cm³, showed that the settlement soil layer, pile stress, and pile-top displacement varied with the variation of surcharge load on the soil surface. According to the results, the neutral plane of a single pile shifted from 0.8 to 0.95 L (where L is the length of the pile in sand) as the surcharge load increased from 20 to 120 kPa. Applying a load to the pile head reduced NSF compared to surcharge only conditions, but the elevation of the neutral plane increased [16].

Artificial collapsible soil was prepared by mixing sand and kaolin with different water contents to achieve different collapse potentials (18, 9, 4.2, and 12.5 %). It was used to investigate the variation of NSF under different inundation pressures, degrees of saturation, and directions of inundation. The results showed that the collapse potential as well as the degree of saturation significantly affected NSF along the end-bearing pile shaft. Bottom-up inundation resulted in a higher neutral plane elevation than top-down inundation. To verify the results obtained during the experimental work, a numerical model was created in the PLAXIS 2D program [17].

Recently, China has been building high-rise buildings on collapsible soils (loess soils), which account for about 6.6% of the country's total area. That is why the collapsibility of the loess soil layer should not be ignored. Therefore, the use of a pile foundation is more suitable for transferring loads to deeper, stable layers. But the loess soil softens upon water immersion, producing additional downward pressure and settlement on the pile. This prompted the researchers to study the effect of cumulative relative collapse amount, the influence of pile type, and the effect of collapsibility change on the NSF with water immersion. The small relative displacement between the pile and the surrounding soil is enough to generate large NSF. Driven precast piles exhibited higher maximum NSF than that of the bored concrete pile due to compaction and surcharge surface loading. Bored concrete piles showed rapid NSF development and the variation in collapsibility of loess soil due to the changing of both natural water content and dry density. Finally, surcharge loading and pre-wetting could reduce NSF [18].

In [19], NSF along the shaft of two types of piles was calculated using a laboratory model: floating pile and end-bearing pile in gypseous soil (with 42% gypsum content) from the Bahr Al-Najaf region, Iraq. The researchers found that the final settlement for the end-bearing pile is less than that for the floating pile with the same degree of saturation. But the maximum value of NSF for the end-bearing pile is smaller than that for the floating pile due to differences in soil-pile relative displacement. A scale model was used to investigate the variation and the distribution of NSF on piles in loess soil. The results showed that the loess soil exhibited layered settlement under immersion conditions, as well as negative and positive friction on the pile surface and two neutral sites. Negative friction pulls the pile downward, increasing the axial force of the pile. Higher soil elastic modulus at the pile tip increased maximum NSF and lowered the neutral point position. By representing the laboratory model through a numerical model, it was found that the results were close to the experimental ones [20].

The collapsible gypseous soil covers 20–30% of Iraq's landmass and is distributed in the northwest, west, and southwest regions of Iraq, with gypsum content exceeding 60 % in some regions [21, 22].

The aim of this study is to evaluate NSF along the shaft of a pile embedded in gypseous soil by using a laboratory model and to study the effect of different parameters on the development of drag load along the shaft of piles, such as collapse potential, soil density, and degree of saturation.

2. Methods

2.1. Laboratory Model

The model used in this study consisted of an iron tank box with dimensions of 80×80×80 cm, manufactured from a 6-mm-thick iron plate and an iron frame. A mechanical jack was employed to conduct a pile load test, determining the allowable load after assuming the factor of safety according to the scientific standards. Moreover, the applied load was measured using an S-shaped load cell with a capacity of 2 tons. The bottom of the box featured three openings to allow water to enter the soil, connected to a water tank positioned 30 cm above the surface of the final soil layer, as shown in Fig. 1.

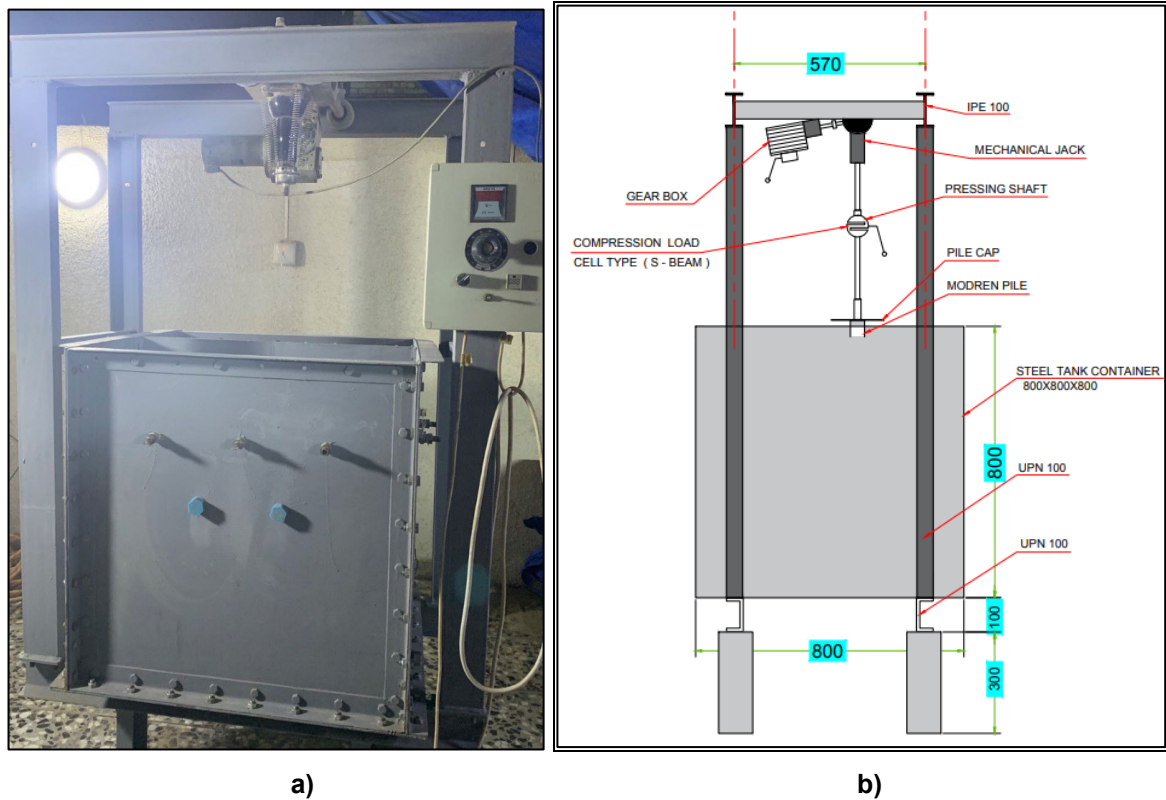


Figure 1. Laboratory model: a) steel box container, b) sketch for laboratory model.

2.2. Soil Used

Gypseous soil that was used in this study was brought from Tikrit city, Iraq. This soil had the following chemical composition:

- gypsum content – 60 %;
- SO_3 – 28 %
- CL – 0.032 %;
- organic content – 0.51 %;
- T.S. S – 77 %;
- pH – 8.25 %.

It was sieved through No. 10 before use. The soil characteristics are listed in Table 1, and the grain size distribution is shown in Fig. 2.

Table 1. Properties of gypseous soil.

Properties	Value	Specification
Soil classification	SM	USCS
Gypsum content	60 %	[23]
Liquid limit	26 %	ASTM 423-66
Plastic limit	Non-plastic	ASTM D424-59
Max dry density	17 kN/m ³	ASTM 698-00a
Optimum water content	12.5%	ASTM 698-00a
Cohesion	18 kPa	ASTM D3080-89
Angle of internal friction at field density	40°	ASTM D3080-89
	12.7 kN/m ³	
Specific gravity with water	2.39	ASTM D854-02
Specific gravity with kerosene	2.37	Manual of soil laboratory testing ¹

¹ Head, K.H. Manual of Soil Laboratory Testing. 1. Pentech Press. London, 1980. 422 p.

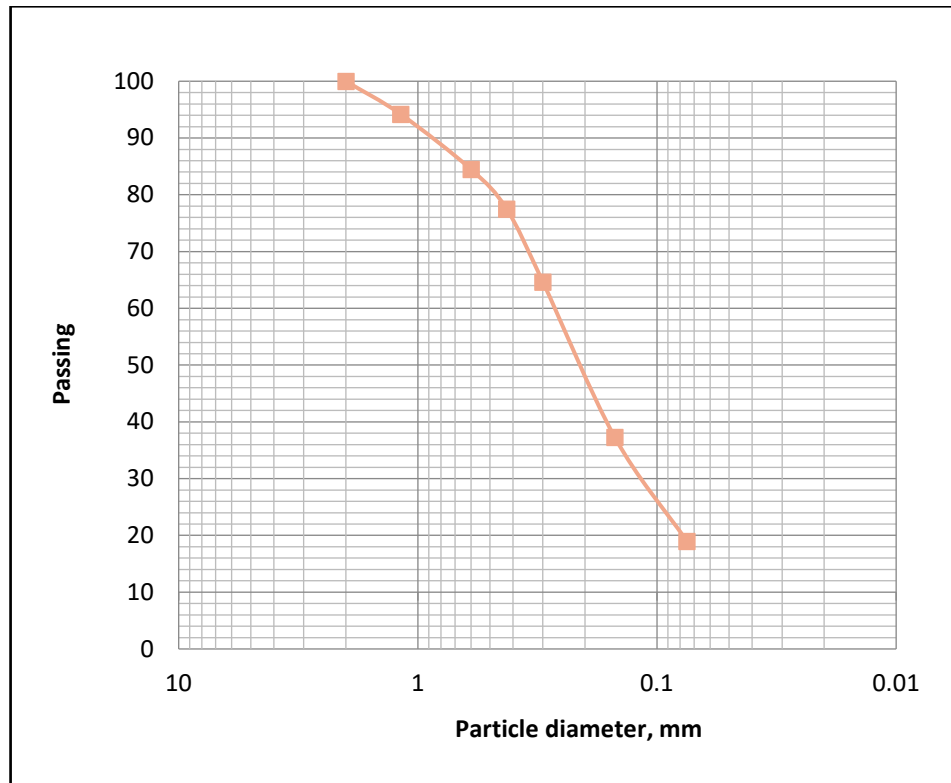


Figure 2. Grain size distribution curve of gypseous soil.

2.3. Properties of the Pile, Strain Gauge, and Load Cell

Two types of steel piles with different lengths, 30 and 20 cm, with an outer diameter of 2.1 cm and an inner diameter of 1.95 cm, were used. The surface of these piles was roughened by a knurling machine to ensure full friction between the pile and soil. The 30-cm-long pile was provided with eight electrical strain gauges of the Rosette type and fixed at positions 5, 10.5, 19.5, and 29.5 cm from the top of the pile. Similarly, the 20-cm-long pile was equipped with six strain gauges positioned at 5, 10.5, and 19.5 cm from the top of the pile as shown in Fig. 3.

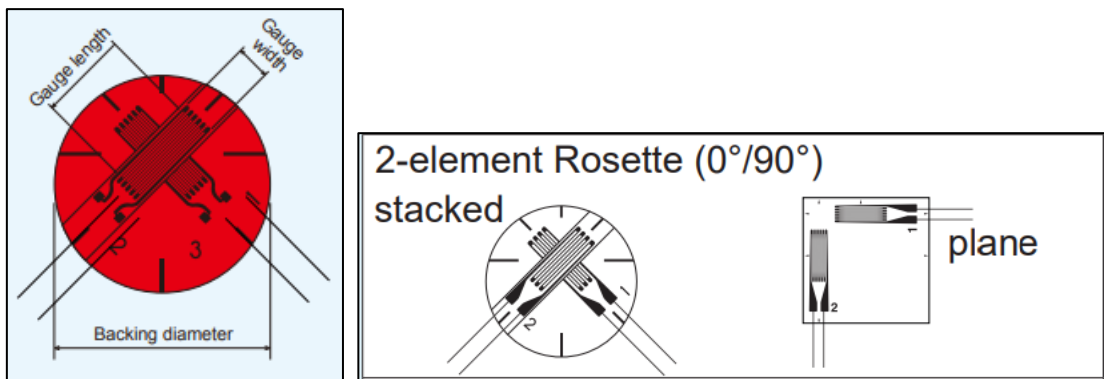


Figure 3. Strain gauge Rosette and its distribution along the pile.

The properties of the strain gauges are shown in Table 2.

Table 2. Properties of strain gauges².

Gauge length	Gauge resistance	Gauge factor
3 mm	118.5±0.5Ω	2.08±1

Each Rosette has two strain gauges arranged perpendicularly and bonded with a specialized adhesive. After installation, the strain gauges were coated with a special coating material (W-1), and wrapped with SB-type tape to ensure waterproofing. At the end of each pile, a load cell with 50 kg capacity was used to calculate the end-bearing resistance. This load cell was placed within an iron chamber and was attached to the pile using rubber tape of an appropriate type as shown in Fig. 4.

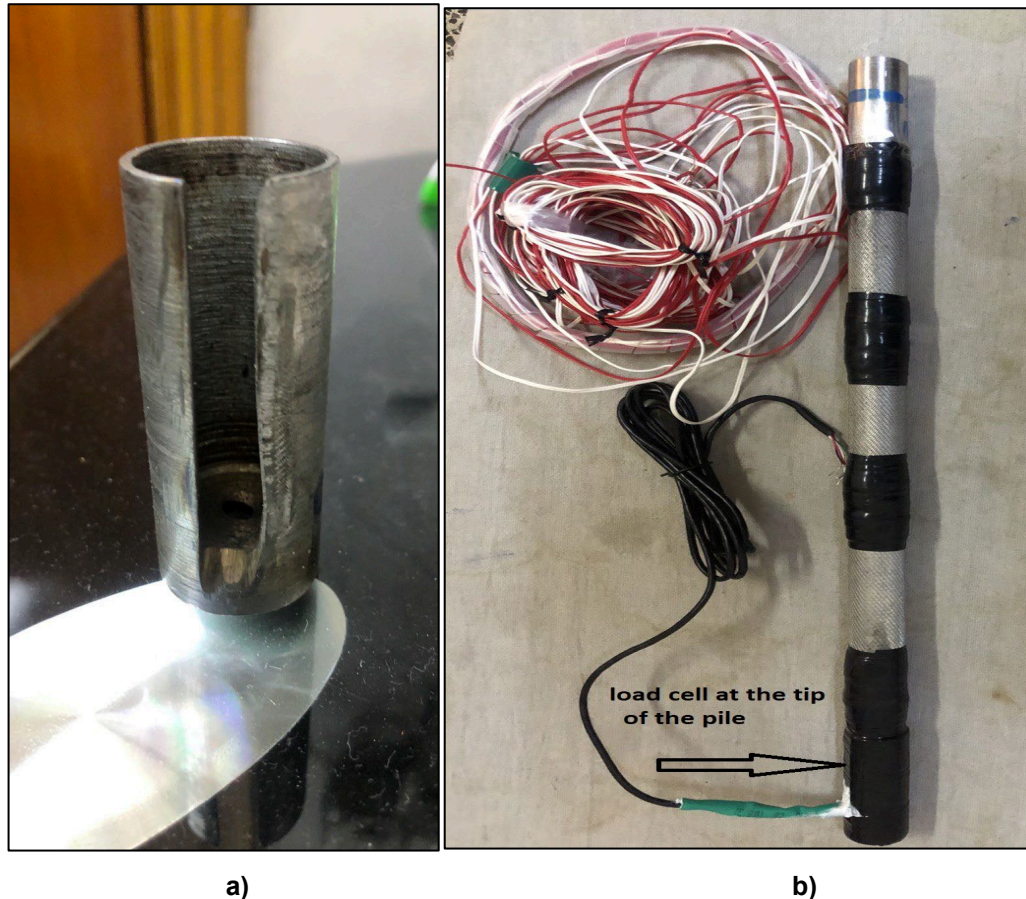


Figure 4. 50 kg-capacity load cell measuring end-bearing resistance: a) iron chamber for the load cell, b) load cell at the tip of the pile inside the chamber.

2.4. Methodology

Due to the fact that the fine materials percentage in the soil used in this study (gypseous soil) is high, the compaction curve in Fig. 5 was used to estimate the dry unit weight for the collapse tests, enabling a more accurate study of pile behavior in gypseous soil during inundation. The collapse potential values for each dry unit weight, obtained from a single collapse test [24], are shown in Table 3. Based on the results obtained, four dry unit weights have been adopted as shown in Table 3. It is important to note that the severity of the gypseous soil's collapsibility was characterized according to [24].

² Tokyo Measuring Instruments Laboratory Co., Ltd. [Online]. URL: https://www.tml.jp/eng/documents/Catalog/straingauge2023-2024_E1007H_web.pdf (date of application: 17.07.2025)

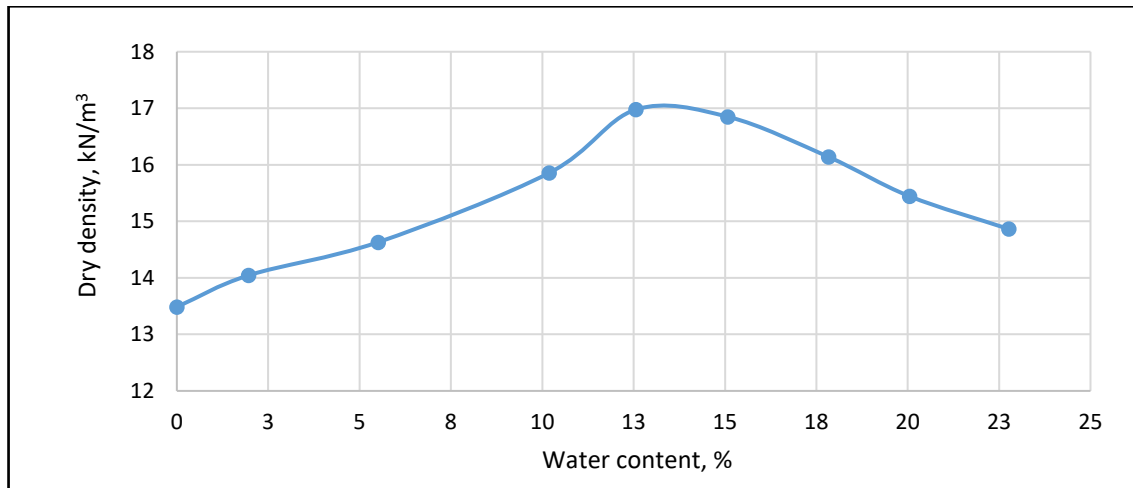


Figure 5. Compaction curve of the used soil.

Table 3. Results of the single collapse test.

Degree of saturation, %	Water content, %	Dry unit weight, kN/m ³	Collapse potential, %
0	0	13.5	11.4
5	1.5	14	9.9
10	3	14.2	9.5
15	4.2	14.4	8.6
20	5.1	14.6	6.5
25	6.2	14.9	5.3
30	7.2	15	3.8
35	8	15.2	2.9
45	9.6	15.5	2.9
60	11	16.1	0.28
80	12.6	17	0.28
90	15	17	0.28

*The highlighted values have been considered in the tests of NSF on piles as initial test conditions

After determining the required densities for layering the gypseous soil in the laboratory model, a 10-cm-thick layer of gravel was placed at the bottom of the model. Then, the soil was layered to a 50 cm height using a hand hammer, during which each board pile was installed according to its embedded length in the gypseous soil. A surcharge load of 4 kPa was applied to the soil surface and around the piles to represent the top soil layer in field conditions.

Prior to testing, LVDTs were placed on each pile and on the soil surface to record the settlement. All strain gauges, the load cell at the tip of the pile, and LVDTs were connected to a data logger and computer system to monitor and record data during the test.

Typically, the test began by immersing the lower gravel layer through the holes in the bottom of the model. Once the water has submerged the gravel layer, the bottom water supply was closed, and inundation commenced from the top until full soil saturation was achieved. This inundation procedure simulated various field conditions including rainfall, surface runoff, irrigation, poor drainage, and flooding. Test data were recorded throughout the process, as illustrated in Fig. 6. The time required for the test was 2 days.

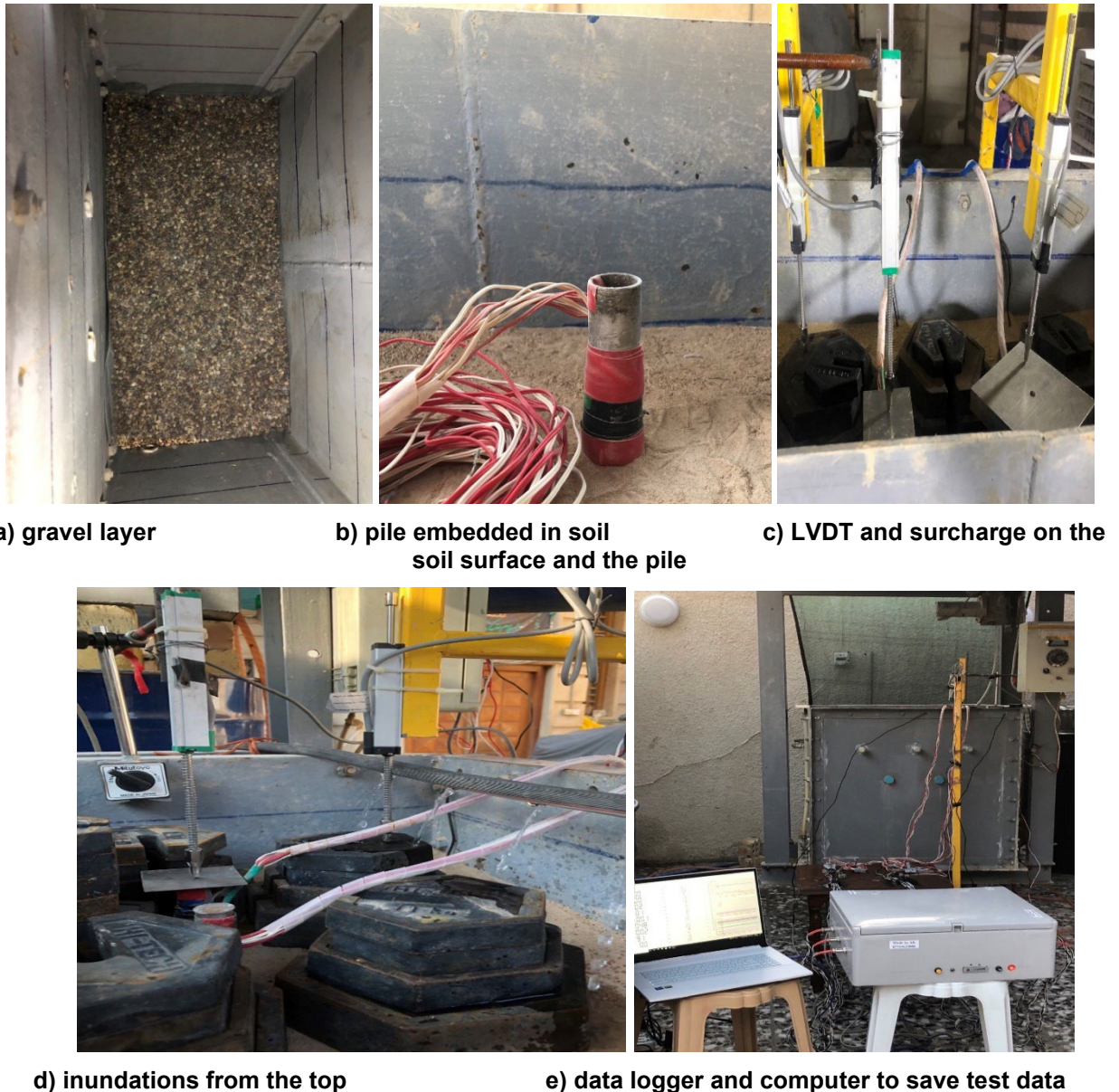


Figure 6. Preparation of the NSF model test.

3. Results and Discussion

The presence of NSF in pile foundation in collapsible soil is a significant source of concern during construction and design due to:

1. Drag load (additional force) generated by NSF and its impact on the pile strength.
2. Additional settlement (drag settlement) caused by NSF and its effect on the design limitation of settlement.

For end-bearing piles, NSF influences the structural pile capacity because the soil beneath the pile is stable (e.g., rock or dense sand). In the floating pile, the effect of NSF must be taken into account in the design processes for both structural and geotechnical pile capacity. It should be noted that considering the drag force as a result of negative friction (an external force) is incorrect, leading to overly conservative calculations in the design. Therefore, it must be treated as an internal force developing within a static equilibrium soil pile system under some conditions [26].

3.1. Relationship between NSF and Collapse Potential

The collapse potential of gypseous soil decreases with an increase in the water content [15]. As presented in Table 3, four values of collapse potential (11.4, 9.6, 8.6, and 5.3 %) were selected corresponding to the dry unit weights (13.5, 14, 14.4, and 14.9 kN/m³, respectively). As shown in Figs. 7–9, NSF resistance increases with increased collapse potential, while no NSF occurs at a collapse potential

of 5.6 % and dry unit weight of 14.9k N/m³ as shown in Fig. 10 for both pile lengths. The collapse potential had a sufficient influence on the drag load development on the pile shaft due to the soil collapse during inundation [17]. During inundation, the bonds break and the soil strength is lost due to the reduction of cementing action of gypsum under wetting. NSF magnitude correlates directly with pile embedment length. The depth, at which the shear stress along the pile shaft transitions from NSF to positive shaft resistance, when the relative displacement between the pile and surrounding soil is zero, is called the neutral plane [26]. It typically occurs in the lower third of the pile [6, 28]. In addition, 30-cm-length pile at the collapse potential of 9.6 and 8.6 % showed two neutral planes, which agrees with [4].

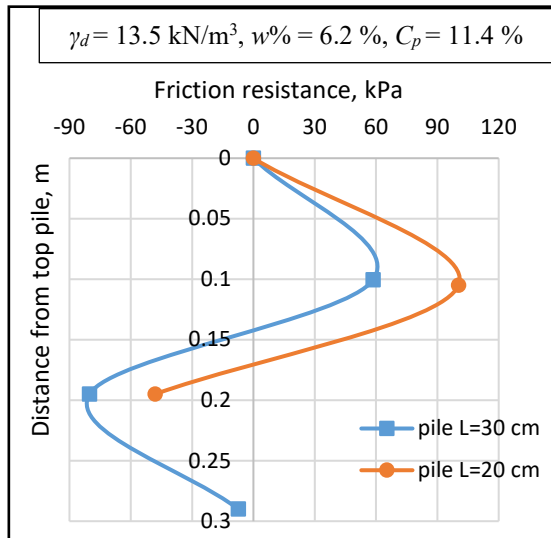


Figure 7. NSF along the shaft of the pile.

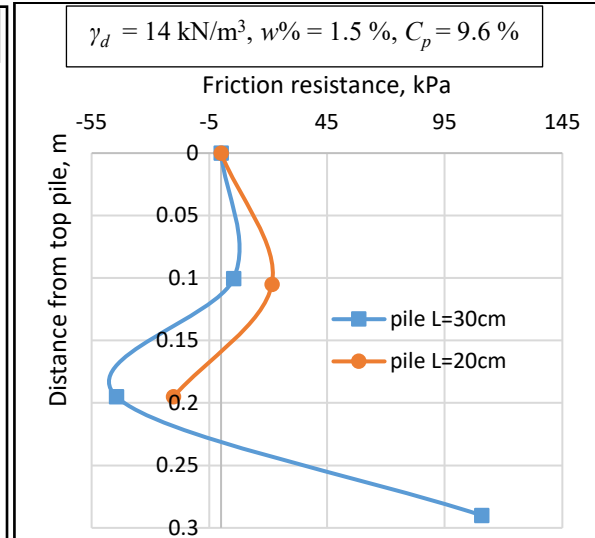


Figure 8. NSF along the shaft of the pile.

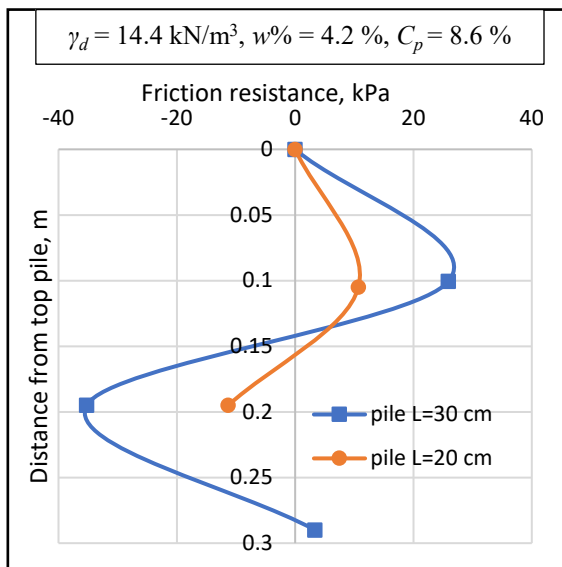


Figure 9. NSF along the shaft of the pile.

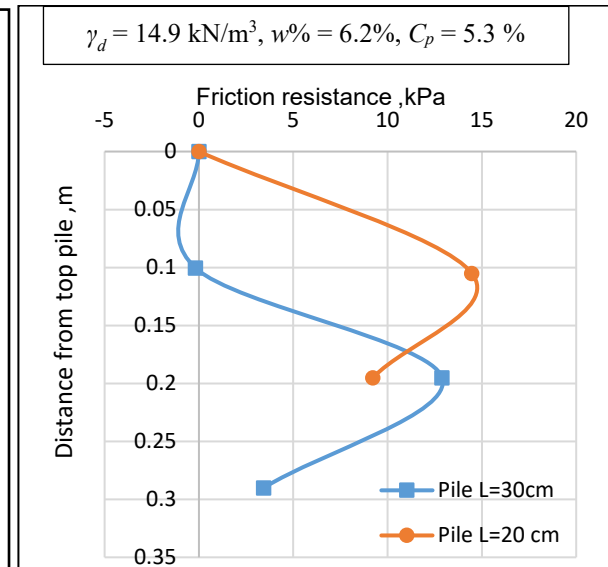


Figure 10. NSF along the shaft of the pile.

3.2. Relationship between Drag Load, Dry Density and Degree of Saturation

Gypseous soil has significant collapse potential due to its metastable structure, which has a low dry density and moisture content. In other words, large volume changes and sudden collapses occur when the soil is soaking [27–29]. As shown in Fig. 11, maximum drag load (peak NSF) increases with a decrease in the degree of saturation and decreases with an increase in the dry density of soil due to a high decrease in the void ratio of soil, which can occur with compaction. The maximum drag load occurs at zero saturation.

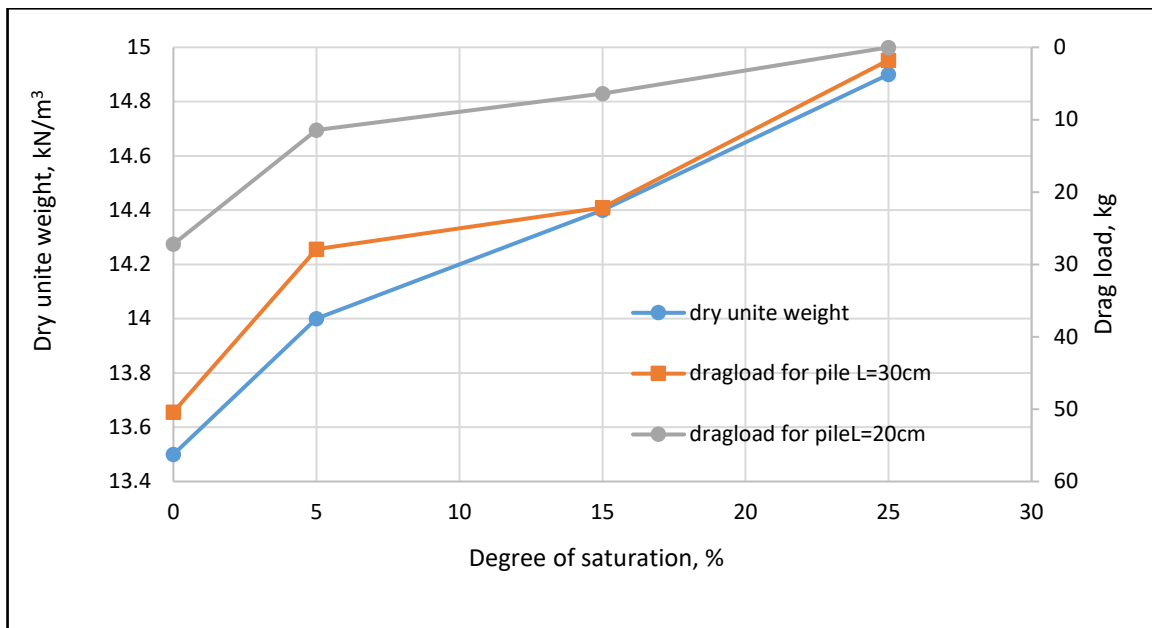


Figure 11. Variation of drag load with dry unit weight and degree of saturation.

3.3. Relationship between Drag Load, Soil Settlement and Pile Settlement

NSF generation primarily results from soil-pile relative settlement. Extremely small movement (≥ 1 mm) can cause NSF force and reverse the shear-force direction along the shaft of the pile [6]. Moreover, large deformations and rapid settlement can occur because of the cemented gypsum bond dissolution during inundation. The relative settlement between soil and pile is high at zero degree of saturation, while 25% saturation produces insufficient relative movement to generate NSF as shown in Figs. 12–15. The soil displacement near the bottom of the pile is smaller than or equal to the pile displacement, which produces positive skin friction along the shaft. Therefore, soil-pile relative settlement of about 1–3 mm (for a long pile) and about 1–2.5 mm (for a short pile) is enough to generate a drag load on the pile in the gypseous soil.

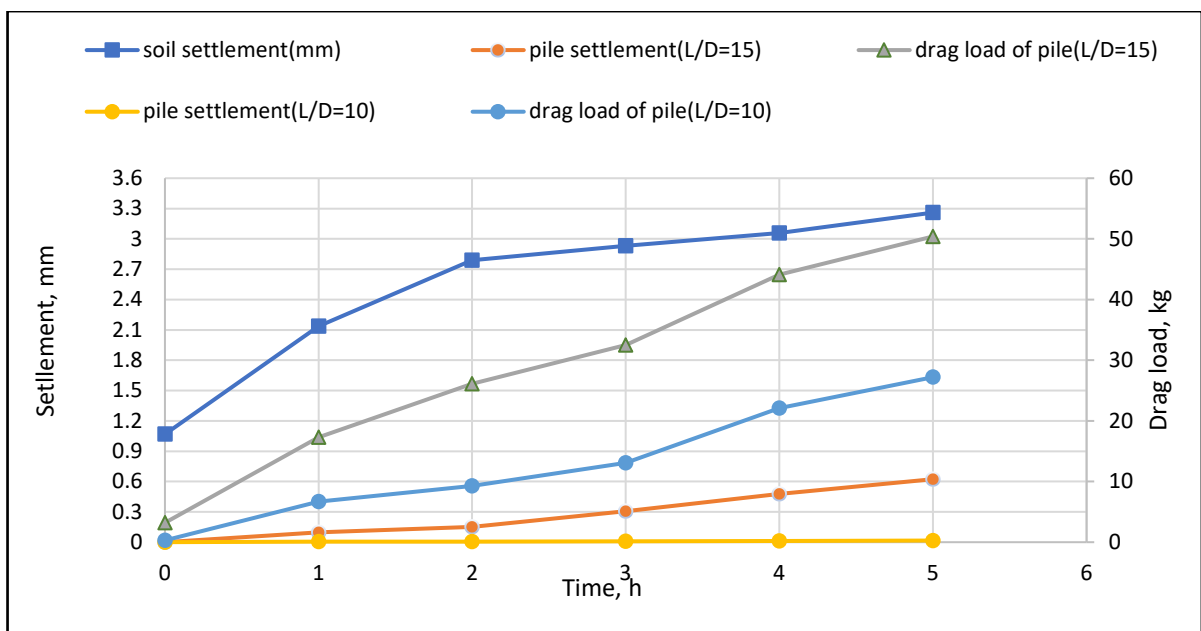


Figure 12. Variation of the settlement of pile and soil with drag load force for $C_p = 11.4\%$.

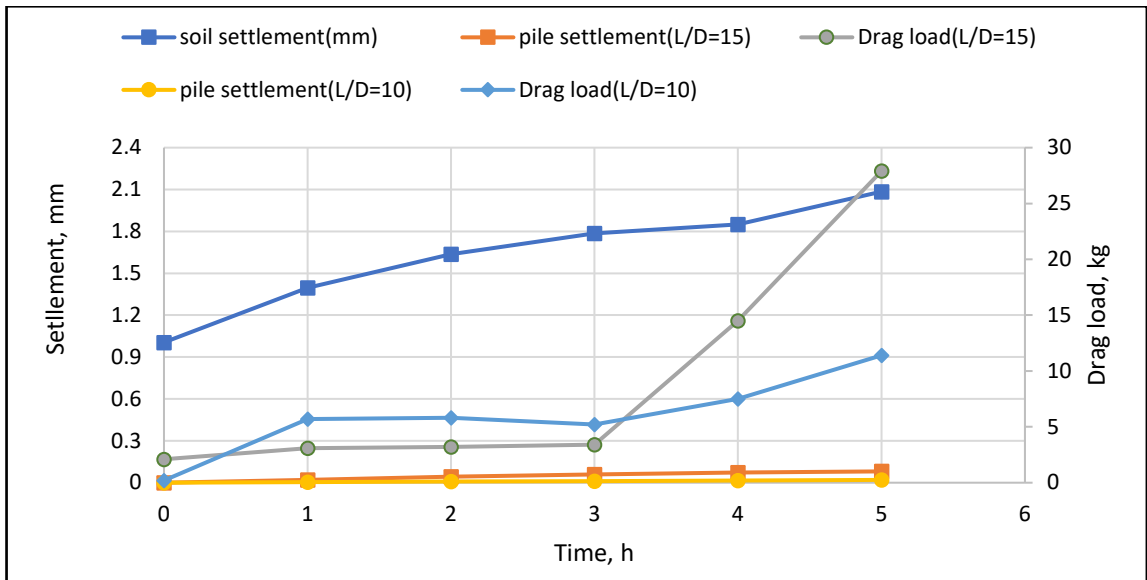


Figure 13. Variation of the settlement of pile and soil with drag load force for $C_p = 9.6\%$.

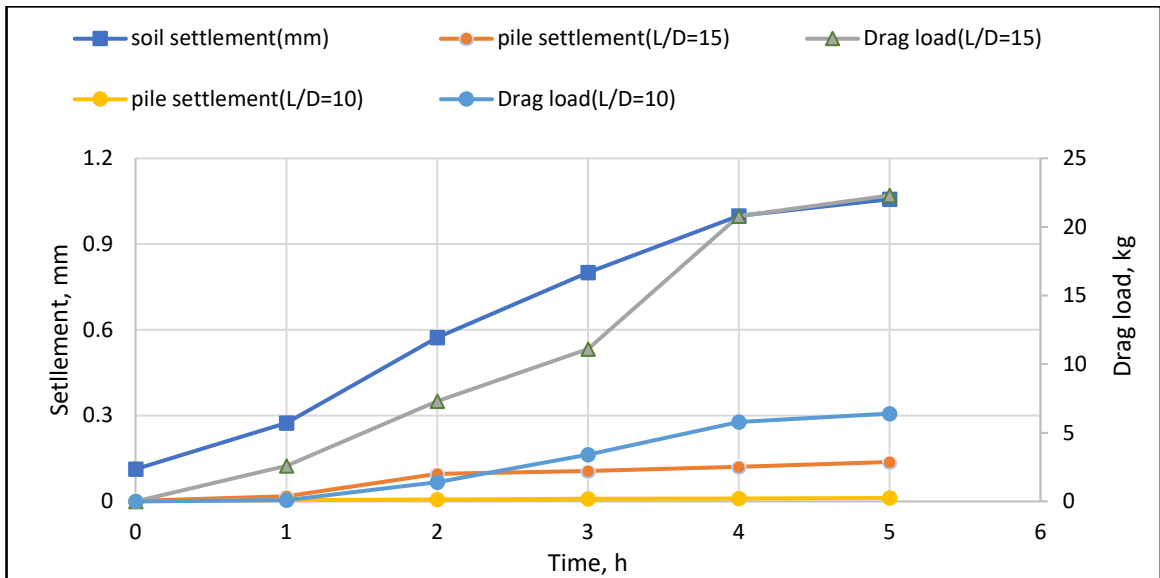


Figure 14. Variation of the settlement of pile and soil with drag load force for $C_p = 8.6\%$.

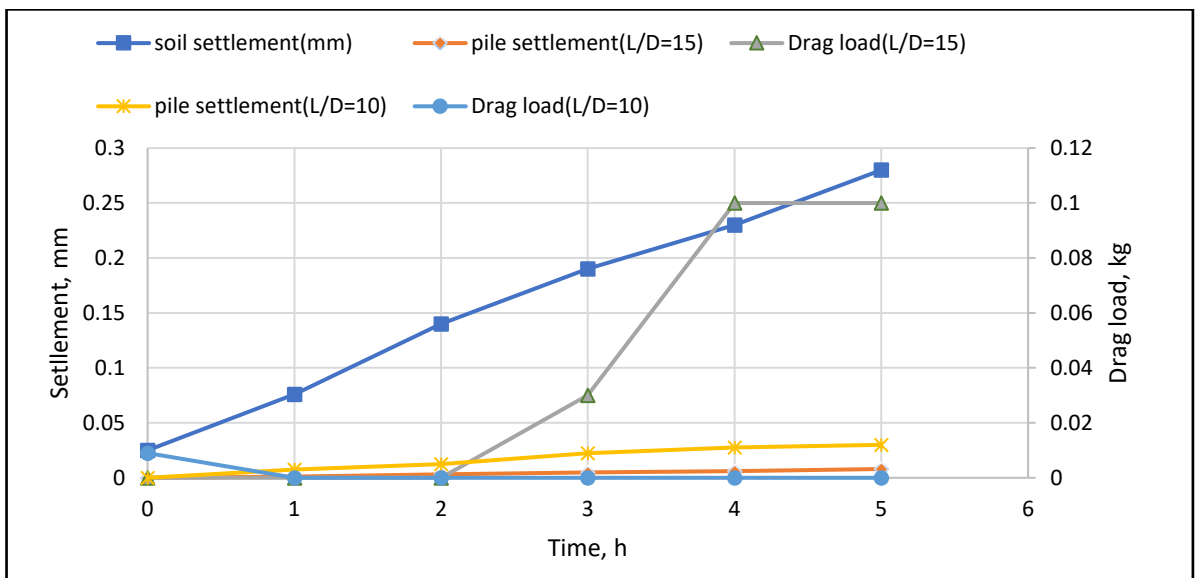


Figure 15. Variation of the settlement of pile and soil with drag load force for $C_p = 5.3\%$.

4. Conclusion

The article examined the development of NSF along the shaft of the pile during the gypseous soil inundation using a physical model, gypseous soil, and piles with two distinct length/diameter (L/D) ratios. The following conclusions can be obtained based on the results:

1. Submergence of gypseous soil samples with varying densities and water contents alters collapse potential values. In other words, not all collapse potential values are sufficient to produce NSF, therefore, the recommended safety factor during the design process will change as the drag load is developed along the pile shaft.
2. Piles with a slenderness ratio $L/D = 15$ exhibit substantially higher NSF resistance than those with $L/D = 10$, attributed to increased soil-pile interaction area. NSF resistance increases by 66, 119, and 211% for collapse potentials of 11.4, 9.9, and 8.6%, respectively.
3. In its natural state, gypseous soil has a high void ratio and a low dry density. The cementation bonds will break up during inundation, increasing the compressibility of gypseous soil. Accordingly, when soil is compacted at a high dry density, the void ratio in the soil decreases, which lowers the soil's ability to collapse, and water cannot easily dissolve the cementing bonds between the soil particles.
4. For pile length = 30 cm, NSF resistance increases by 26% when the degree of saturation decreases from 20 to 5% and by 60% when the degree of saturation decreases from 5 to 0%, respectively. For pile length = 20 cm, NSF resistance increases by 78% when the degree of saturation decreases from 20 to 5% and by 137% when the degree of saturation decreases from 5 to 0%, respectively.

References

1. Abd-Alhameed, H.J., Albusoda, B.S. Impact of eccentricity and depth-to-breadth ratio on the behavior of skirt foundation rested on dry gypseous soil. *Journal of the Mechanical Behavior of Materials*. 2022. 31(1). Pp. 546–553. DOI: 10.1515/jmbm-2022-0057
2. Noor, S.T., Hanna, A., Mashhour, I. Numerical Modeling of Piles in Collapsible Soil Subjected to Inundation. *International Journal of Geomechanics*. 2013. 13(5). Pp. 514–526. DOI: 10.1061/(ASCE)GM.1943-5622.0000235
3. Huang, T., Gong, W.M., Dai, G.L., Zheng, J.H., Xu, G. P. Experimental study of time effect of negative skin friction on pile. *Rock and Soil Mechanics*. 2013. 34(10). Pp. 2841–2846.
4. Ye, S., Zhao, Z., Zhu, Y. Study on negative friction of pile foundation in single homogeneous soil layer in collapsible loess area of Northwest China. *Arabian Journal of Geosciences*. 2021. 14. Article no. 1137. DOI: 10.1007/s12517-021-07508-2
5. Bjerrum, L., Johannessen, I.J., Eide, O. Reduction of negative skin friction on steel piles to rock. *Proceedings of the 7th International Conference on Soil Mechanics and Foundation Engineering*. Mexico City, 1969. 2. Pp. 27–34.
6. Fellenius, B.H., Broms, B.B. Negative skin friction for long piles driven in clay. *Proceedings of the 7th International Conference on Soil Mechanics and Foundation Engineering*. Mexico City, 1969. 2. Pp. 93–98.
7. Fellenius, B.H. Down-drag on Piles in Clay due to Negative Skin Friction. *Canadian Geotechnical Journal*. 1972. 9(4). Pp. 323–337. DOI: 10.1139/t72-037
8. Fellenius, B.H. Unified design of piles and pile groups. *Transportation Research Record*. 1989. Article no. 1169. Pp. 75–82.
9. Grigoryan, A.A. Construction on loess soils. *Soil Mechanics and Foundation Engineering*. 1991. 28. Pp. 44–49. DOI: 10.1007/BF02304644
10. Thomas, J., Fahey, M., Jewell, R. Pile down-drag due to surface loading. *Centrifuge 98*. 1998. 1. Pp. 507–512.
11. Lee, C.J., Chen, C.R. Negative Skin Friction on Piles Due to Lowering of Groundwater Table. *Journal of the Southeast Asian Geotechnical Society*. 2003. 34(1). Pp. 13–25.
12. Leung, C.F., Liao, B.K., Chow, Y.K., Shen, R.F., Kog, Y.C. Behavior of Pile Subject to Negative Skin Friction and Axial Load. *Soils and Foundations*. 2004. 44(6). Pp. 17–26. DOI: 10.3208/sandf.44.6_17
13. Feng, Z., Hu, H., Zhao, R., He, J., Dong, Y., Feng, K., Zhao, Y., Chen, H. Experiments on Reducing Negative Skin Friction of Piles. *Advances in Civil Engineering*. 2019. 2019. Article no. 4201842. DOI: 10.1155/2019/4201842
14. Houston, S.L., Houston, W.N., Zapata, C.E., Lawrence, C. Geotechnical engineering practice for collapsible soils. *Geotechnical and Geological Engineering*. 2001. 19. Pp. 333–355. DOI: 10.1023/A:1013178226615
15. Al-Mufti, A.A. Effect of gypsum dissolution on the mechanical behavior of gypseous soils. PhD thesis. Baghdad, 1997.
16. Huang, T., Zheng, J., Gong, W. The Group Effect on Negative Skin Friction on Piles. *Procedia Engineering*. 2015. 116. Pp. 802–808. DOI: 10.1016/j.proeng.2015.08.367
17. Mashhour, I. Experimental study on negative skin friction on piles in collapsible soils due to inundation. PhD thesis. Montreal, 2016.
18. Xing, H., Liu, L. Field Tests on Influencing Factors of Negative Skin Friction for Pile Foundations in Collapsible Loess Regions. *International Journal of Civil Engineering*. 2018. 16(10). Pp. 1413–1422. DOI: 10.1007/s40999-018-0294-z
19. Al-Damluji, O.A., Albusoda, B.S., Ali, A.H. Performance evaluation of a model pile in gypseous soil. *Proceedings of the 16th Asian Regional Conference on Soil Mechanics and Geotechnical Engineering (16ARC 2019)*. Taipei, 2019. Pp. 14–18.
20. Zhao, Z., Ye, S., Zhu, Y., Tao, H., Chen, C. Scale model test study on negative skin friction of piles considering the collapsibility of loess. *Acta Geotechnica*. 2022. 17. Pp. 601–611. DOI: 10.1007/s11440-021-01254-1
21. Albusoda, B.S., Salman, R. Bearing Capacity of Shallow Footing on Compacted Filling Dune Sand Over Reinforced Gypseous Soil. *Journal of Engineering*. 2013. 19(5). Pp. 532–542. DOI: 10.31026/j.eng.2013.05.01

22. Mohsen, A.H., Albusoda, B.S. The Collapsible Soil, Types, Mechanism, and identification: A Review Study. Journal of Engineering. 2022. 28(5). Pp. 41–60. DOI: 10.31026/j.eng.2022.05.04
23. Al-Muftay, A.A.-E., Nashat, I.H. Gypsum content determination in gypseous soils and rocks. Proceedings of the 3rd Jordanian International Mining Conference. Amman, 2000. 2. Pp. 485–492.
24. American Society for Testing and Materials (ASTM). Standard Test Method for Measurement of Collapse Potential of Soils. ASTM D5333-92. ASTM. West Conshohocken, 1996. 3 p. DOI: 10.1520/D5333-92R96
25. Pells, P., Robertson, A., Jennings, J.E., Knight, K. A guide to construction on or with materials exhibiting additional settlement due to "collapse" of grain structure. International Journal of Rock Mechanics and Mining Sciences & Geomechanics Abstracts. 1975. 12(9). P. 131. DOI: 10.1016/0148-9062(75)91203-61975
26. Aram, A. Analysis of Piles for Negative Skin Friction. Fourth Year Project. 2010. URL: <https://www.scribd.com/document/149135616/analysis-of-piles-for-negative-skin-friction> (date of application: 22.07.2025).
27. Nashat, A.A., Ludeman, L.C. Detection and estimation of chirp signals using state space representation. 1992 IEEE International Symposium on Circuits and Systems (ISCAS). San Diego, 1992. 3. Pp. 1609–1612. DOI: 10.1109/ISCAS.1992.23018
28. Sasam, S.I., Alsaidi, A.A., Mukhlef, O.J. Behavior of Reinforced Gypseous Soil Embankment Model under Cyclic Loading. Journal of Engineering. 2013. 19(7). Pp. 830–844. DOI: 10.31026/j.eng.2013.07.05
29. Albusoda, B.S., Alahmar, M.M. The Behavior of Gypseous Soil under Vertical Vibration Loading. Journal of Engineering. 2014. 20(1). Pp. 21–30. DOI: 10.31026/j.eng.2014.01.02

Information about the authors:

Abeer Mohsen,

ORCID: <https://orcid.org/0009-0009-7697-2926>

E-mail: Abeer.mohsin2001D@coeng.uobaghdad.edu.iq

abeer.h.mohsen@src.edu.iq

Bushra Suhale Albusoda,

ORCID: <https://orcid.org/0000-0001-6375-4430>

E-mail: dr.bushra_albusoda@coeng.uobaghdad.edu.iq

Received: 17.12.2022. Approved: 15.09.2024. Accepted: 15.03.2025.